PROTOTYPING, TESTING AND PERFORMANCE OF THE TWO-STAGE SEISMIC ISOLATION SYSTEM FOR ADVANCED LIGO GRAVITATIONAL WAVE DETECTORS

Fabrice Matichard[1,2], Richard Mittleman[1], Brian Lantz[3], Ben Abbott[2], Sam Barnum[1], Dennis Coyne[2], Dan DeBra[3], Stephany Foley[1], Joseph Giaime[4], Corey Gray[5], Joe Hanson[4], Jeff Kissel[6], Myron MacInnis[1], Ken Mason[1], Brian O'Reilly[4], Hugh Radkins[5], Céline Ramet[4], David Shoemaker[1], Andy Stein[1].

[1]LIGO, MIT
Cambridge, MA, US.
[2]LIGO, Caltech
Pasadena, CA, US.
[3]Stanford University, Ginzton Laboratory, Stanford, CA, US.

[4]LIGO Livingston Observatory
Livingston, LA, US.
[5]LIGO Hanford Observatory
Richland, WA, US.
[6]Lousiana State University
Baton Rouge, LA, US.

1. INTRODUCTION

The goal of LIGO is to detect and analyze the gravitational waves produced by astrophysical events [1]. LIGO consists of 4 km scale interferometric detectors located in Washington (LIGO Hanford Observatory, LHO) and Louisiana (LIGO Livingston Observatory, LLO) [2]. Gravitational waves appear as differential length changes in the perpendicular arms. To reach the required level of sensitivity (to motions of 10^{-18} m or less), the interferometer test masses must be isolated from several noise sources, including seismic motion, which is dominant at low frequencies. Initial LIGO has searched for signals, but none have yet been identified.

A significant improvement in sensitivity is underway with the pending installation of Advanced LIGO [3] (or aLIGO). Once running at full sensitivity, sources of gravitational are predicted to be regularly detected. A key element in this upgrade is the installation of extremely effective broadband seismic isolation and positioning systems [4-5]. It will include, for every optic, three levels of isolation in series: an external (in air) active isolation and alignment stage with quiet-hydraulic actuators called HEPI [6], an internal (in vacuum) passive/active isolator called ISI (Internal Seismic Isolator) presented in this paper, and predominantly passive multiple pendulums to hold the optics [7].

A multi-stage Internal Seismic Isolation platform will be used to support the beam splitter and each of the test mass optics. The platform should provide an isolation factor of 10 at 0.1 Hz and up to 2000 at 10 Hz. This active/passive system, called BSC-ISI, under development for several years, is made of two stages in series, each controlled in six degrees of freedom (DOF).

This paper presents the prototyping, testing and current performance of the BSC-ISI system supporting a 920 kg total payload (370 kg of optical payload with the remaining 550 kg configured as ballast). In the next section, the BSC-ISI architecture and the prototype are presented. The active control strategy is presented in section 3. Initial performance results and related structural investigation are presented in section 4, followed by improved performance in section 5.

2.BSC-ISI ARCHITECTURE AND PROTOTYPE

A rendering of the BSC Internal Seismic Isolation platform can be seen in figure 1. Either the triple pendulum suspension for the beam splitter or the quadruple pendulum suspension for the test masses (neither are shown) would be suspended from the optical table on the bottom of the second stage.

The base of the system is shown in blue on the CAD model in figure 2. It supports Stage 1, shown in cyan, via blades and flexure rods shown in yellow. The blades provide the vertical flexibility and the rods provide the horizontal one. Stage 1 supports Stage 2, shown in grey, via the same type of blades and flexure rods also shown in yellow. The two suspended stages have natural frequencies in the 1 Hz - 7 Hz range. The system is designed to provide passive isolation above its natural frequencies

and active control isolation in the 0.1 Hz - 20 Hz range.

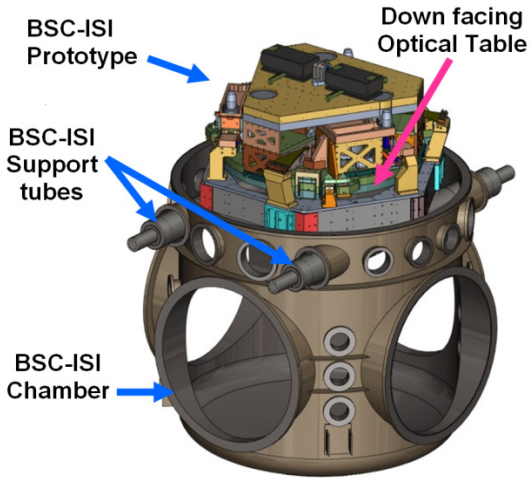

FIGURE 1. Model of the BSC-ISI on its supports tubes at the top of the BSC chamber (doors, dome and flanges not shown)

For the active control, six coarse (high force) electromagnetic actuators are used between the base and stage 1. They are shown in pink on figure 2. Six smaller fine (low force) electromagnetic actuators, also shown in pink on figure 2, are used to actuate between stage 1 and stage 2. The blades, rods and actuators have been designed and positioned to decouple the horizontal and vertical motion of the stages.

Sensors are shown in red on figure 2. Stage 1 is instrumented with three different sets of sensors:
- 6 MicroSense (formerly ADE technologies) capacitive position sensors between the base and stage 1, called "coarse". They are used for low frequency relative positioning.
- 3 Streckeisen STS-2 seismometers: these 3-axis seismometers provide the low frequency inertial measurements necessary to provide active seismic isolation.
- 6 Sercel L-4C geophones: these single-axis seismometers provide the high frequency inertial sensing necessary to provide active seismic isolation at higher frequencies.

Stage 2 is instrumented with two different sets of sensors:
- 6 MicroSense capacitive position sensors between stage 1 and stage 2, called "fine". They provide the low frequency relative positioning.
- 6 Geotech GS-13 seismometers: these single-axis seismometers provide the inertial sensing needed for active seismic isolation.

The prototype installed on the support tubes at the LIGO MIT test facilities is shown in figure 3.

The bottom plate of Stage 2 is the down-facing optical table supporting the optics.

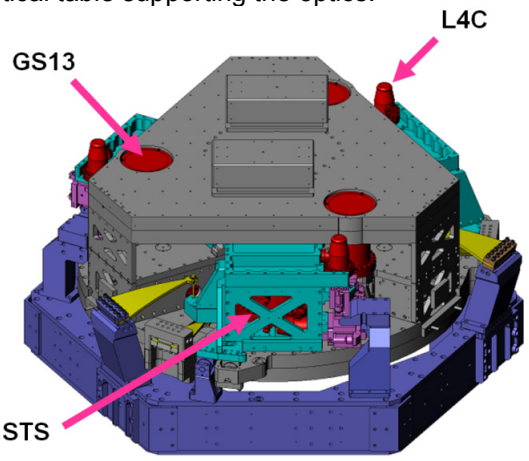

FIGURE 2. CAD model of the BSC-ISI.

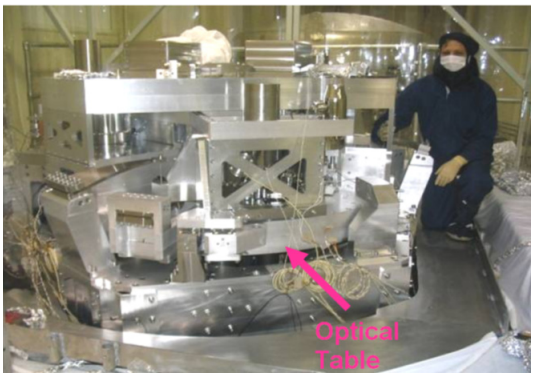

FIGURE 3. The BSC-ISI prototype at LIGO MIT.

3. ACTIVE CONTROL STRATEGY

The feedback control approach is described on the diagram in figure 4.

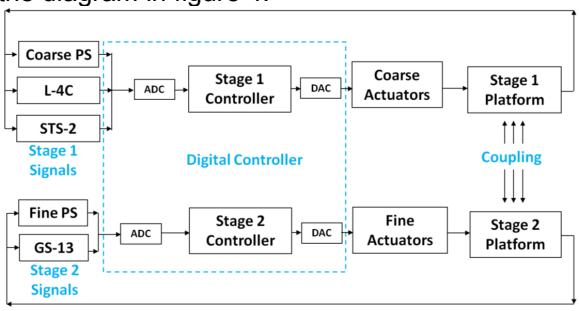

FIGURE 4. Active control general diagram.

It shows the input control signals of stage 1 made of the 6 Position Sensors (PS), 3 three-axis seismometers (STS-2) and 6 single axis seismometers (L-4C). It shows the input control signals of Stage 2 consisting of 6 position sensors (PS), and 6 single-axis seismometers (GS-13).
Those signals are digitized and sent to stage 1 and stage 2 controllers that drive the coarse and fine actuators, respectively. Although stage

motions are coupled to each other, the stages can be controlled independently as explained in the next paragraph which describes the controllers structure.

For each stage, the control is based on the use of 6 independent SISO loops. The control is done in the basis of the General Coordinate System (GCS) of the MIT test facilities: X, Y, RZ, Z, RX, RY. X and Y are aligned with the arms of the interferometer, Z is the vertical axis and RX, RY and RZ the rotations around those axes. The origin of the GCS is on the plan of the coarse horizontal actuators.

Figure 5 shows the block diagram used for each of the 6 digital controllers of each stage. Each SISO controller senses and controls in one direction or one rotation. Firstly, the 6 position sensors of one stage are combined to obtain the motion of this stage in the GCS through a Local to General coordinate change of basis matrix (L2G on block 1 in fig. 5). The same thing is done for the seismometers to get the inertial motion of the stage in the GCS.

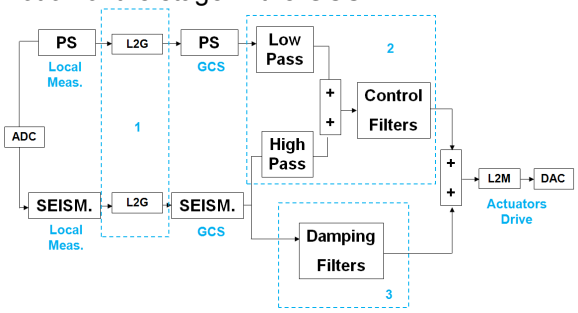

FIGURE 5. Block diagram of one DOF.

The seismometer signal in the GCS is first used to damp the suspension resonances (block 3 on Fig 5). This makes the further developments easier.

Position sensors and seismometers signals are then blended [8]: the position sensors signal is filtered by a low pass and the seismometer is filtered by a high pass. The two signals are summed resulting in a "super sensor" (block 2 on figure 5). The super sensor signal is dominated by relative displacement sensing at low frequency and inertial sensing at high frequency. The frequency at which relative sensing and inertial sensing have equal participation is referred to as the blend frequency (BF).

Finally, a control filter is applied to the super-sensor to provide loop gain. These filters typically are designed for a unity gain frequency (UGF) between 20 Hz and 30 Hz. The control strategy locks the stages to the base below the BF, which provides positioning and alignment capabilities, and drift rejection. The control provides seismic isolation from the BF (around a few tenths of a hertz or below) to the UGF.

4. INITIAL PERFORMANCE RESULTS AND ANALYSIS

Initial performance obtained after the first BSC-ISI commissioning are presented in figure 6. The black curve is the input disturbance (motion of the HEPI system supporting the BSC-ISI). The blue curve shows the motion of stage 2 when the control is off. The system provides passive isolation as expected above 7 Hz. The magenta curve shows the motion of stage 2 with the control on. In this example, the active control improves the isolation between 0.25 Hz and 10 Hz.

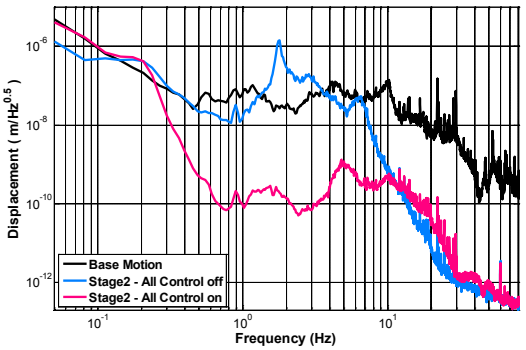

FIGURE 6. Initial performance - Z direction

At low frequencies, one the main factors limiting the performance is the sensitivity of horizontal seismometers to tilt motion. At high frequencies it is limited by the high modal density of the structure and the payload, as seen in the transfer function in figure 7.

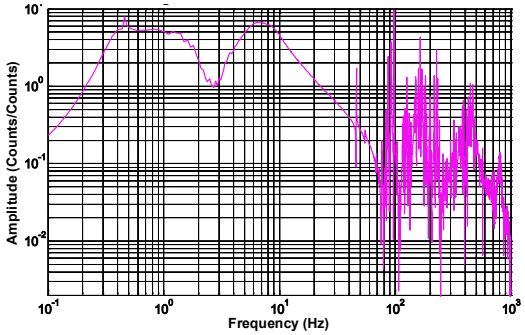

FIGURE 7. Example of transfer functions. Drive X to Sense X with GS13 - Oct 2008.

Initial control results showed that the modal density due to structural resonances needed to be lowered in order to make the control more robust and to improve the performance.

Modal testing investigation identified modes related to the optical payload. The current optical payload under test is a 370 kg system,

whose structural resonances couple to the BSC-ISI. We are currently investigating methods to damp these modes passively. Other sources were identified, such as the counterweights used to balance the system and the seismometer vacuum chambers being mounted improperly resulting in cantilevered masses.

The plot below illustrates an example of structural improvements. The red curve shows the initial transfer functions. The black one shows the transfer functions after the counter weights attachment were re-engineered. These structural modifications significantly improved the control performance as described in section 5.

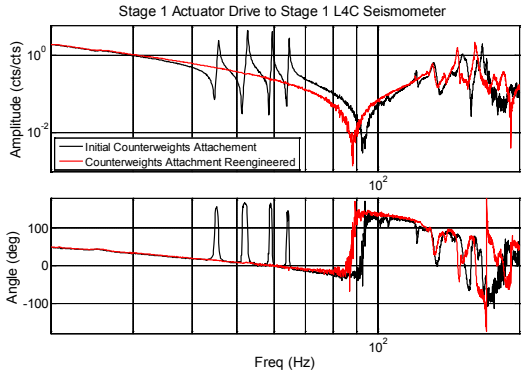

FIGURE 8. Transfer function before and after counterweight attachment reengineering.

5. IMPROVED PERFORMANCE

This section shows the control performance after the structural investigation to improve control robustness and performance. The plot in figure 9 shows the motion of the optical table measured in the X direction with the GS-13s. The black curve shows the motion of the table when the control is off. The blue curve shows the motion of the table under High Frequency Blend (HFB) control on both stages, which is an intermediate control step with reduced isolation. Position sensors and seismometers are blended at 0.7 Hz and the active control provides isolation from 1 Hz to 20 Hz.

Once the system is under HFB control, the "X to RY" and "Y to RX" low frequency couplings induced by position sensors misalignment can be evaluated and minimized. After decoupling, there is less tilt induced by horizontal motion and the blend frequency can be lowered to put the system under Low Frequency Blend (LFB) control. The red curve shows the results after the BF has been lowered to 0.2 Hz on stage 2. The active control provides isolation from 0.25 Hz to 20 Hz.

The purple curve shows the results of implementing a sensor correction. The principle of sensor correction is to sum stage 1 inertial sensing with stage 2 relative displacement sensing, resulting in a low frequency inertial sensing of stage 2. This reduces the gain peaking at the blend frequency.

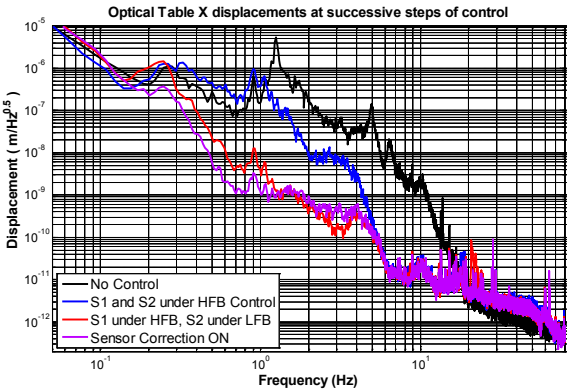

FIGURE 9. Improved performance - X direction.

The next step will be to lower the blend frequency on stage 1 which should provide the same level of improvement as from the blue curve to the red curve. At this stage of commissioning, the system meets isolation expectations for this intermediate level of control:

- At low frequencies (around 0.1 Hz) there is very little motion amplification. This is where there is a risk of gain peaking induced by the relative displacement signal part of the control loop. The sensor correction reduces this gain peaking.
- The isolation starts as low as 0.1 Hz. The tilt in horizontal seismometers will have to be reduced in order to further lower the BF.
- The isolation at 1 Hz is close to a factor of 100. Higher isolation would be at the cost of a higher gain peaking at the BF.
- The unity gain frequency is designed to be 30 Hz. The control provides isolation up to 20 Hz. The phase margin is small in order to maximize the loop gain near 10 Hz (the gain is nearly 10 at 10 Hz). The drawback is higher gain peaking above 20 Hz. This is a good trade-off since the ISI must provide more isolation at 10 Hz than at 20 Hz and above, where the quadruple pendulum provides excellent passive isolation for the final optic.

The same steps have been followed in all of the degrees of freedom and provide similar performance in Y, Z and RZ.

A slightly higher blend frequency is used for the RX and RY rotations around horizontal axes. The RX control performance is presented in figure 10 to illustrate the rotation control performance. The isolation characteristics are similar to those previously described in the other degrees of freedom except for the blend frequency. In this case the BF is set at 0.4 Hz. This provides isolation from 0.5 Hz and above. The reason why the blend frequency is set higher on the rotation control is to reduce the low frequency gain peaking and consequently the tilt motion amplification that would couple with the control of the horizontal seismometers.

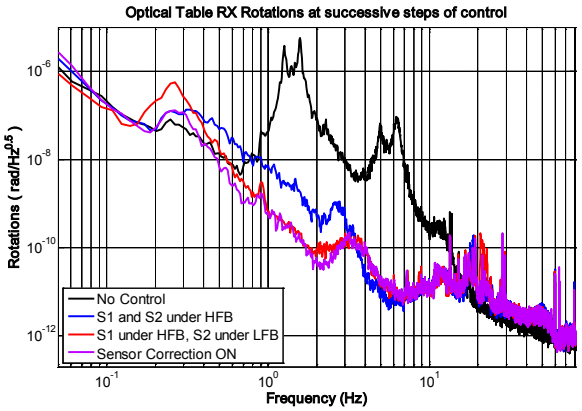

FIGURE 10. RX control performance.

In the previous plots, the control performance was presented (performance with control on versus performance with control off). In the following, we present the overall performance by comparing the motion of the ground with the motion at the top of the piers (BSC-ISI input), the motion of the optical table with control off and the motion of the optical table with control on. The requirement curves are based on aLIGO requirements normalized for the noisier seismic environment of the LIGO MIT urban location.

The performances in the X direction are presented in figure 11:

- The ground motion is shown in black. It is measured with a STS-2 seismometer sitting on the ground 20 feet away from the BSC chamber.

- The motion at the top of the piers is shown in blue. It is measured with HEPI L4Cs.

- The motion of stage 2 when the control is off is presented in red

- The motion of stage 2 when the control is on is presented in purple

- The requirements to be met at MIT in order to meet aLIGO requirement at LLO are presented in grey.

- The requirements to be met at MIT in order to meet aLIGO requirement at LHO are presented in green.

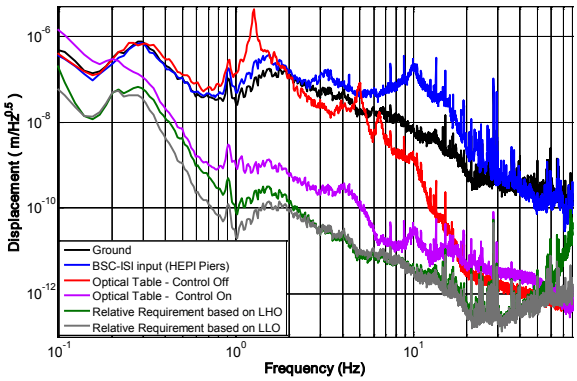

FIGURE 11. BSC-ISI performance – X direction

The blue curve is the input motion of the BSC-ISI system. It is interesting to note that the motion at the top of the chamber is significantly higher than the ground motion. This motion amplification around 10 Hz is due to the motion of the piers driven by the rocking of the vacuum chamber that is heavy enough to rock the ground.

The red curve shows the motion of the optical table when the active control is off. The attenuation from the blue curve to the red one shows the BSC-ISI passive isolation which provides an isolation factor of 100 at 10 Hz and 800 at 20 Hz. The motion of the optical table when the control is on is shown in purple. The system provides a total isolation factor of 6800 at 10 Hz.

The HEPI control and the lower frequency blend that will be implemented on stage 1 is expected to help to meet the requirements from 0.2 Hz to about 8 Hz.

The sensor correction from stage 1 to stage 2 will be adjusted in order to improve the performances around 0.1 Hz. Above 10 Hz it will be difficult to meet the initial requirements. This is not because the BSC-ISI doesn't meet the performance expected by design. It is due to the high input motion at the top of the piers. This is not a critical issue since a recent aLIGO overall noise budget has shown that the seismic noise should be below other sources of noise at those frequencies.

The performance in the vertical direction is presented on figure 12. Like for the horizontal directions, the HEPI control and stage 1 lower frequency blend should help meeting requirements up to about 16 Hz.

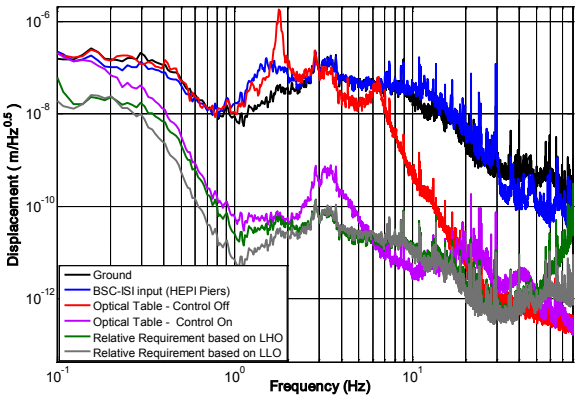

FIGURE 12. BSC-ISI performance – Z direction.

Finally, the plot on figure 13 shows the evolution of the control performance. Each isolation curve consists of the optical table motion when the control is on over the motion when the control is off.

Initial isolation performance, as described in section 4, is shown in black. Current performance is shown in magenta. The slight loss of performance from 0.3 Hz to 0.8 Hz and from 2 Hz to 3 Hz should be largely compensated by the stage 1 blend frequency lowering. This plot shows that the performance around 10 Hz has been improved by a factor of more than 50. It also shows the fine control tuning that is required to minimize the low frequency gain peaking.

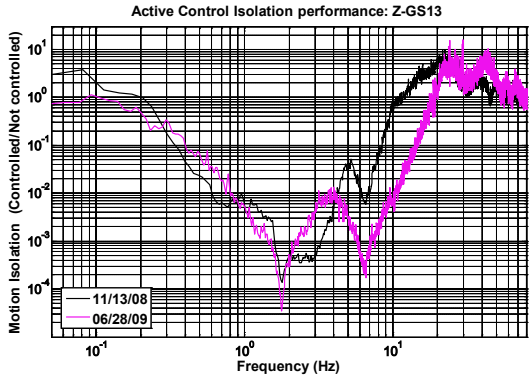

FIGURE 13. Active isolation improvement.

CONCLUSION

The architecture and prototype of the BSC-ISI system, double stage isolation platform that will be used for aLIGO, have been presented. The active control strategy has been described. We presented recent performance measurements of the isolator supporting a 920 kg total payload.

Special attention has been given to the direct correlation between structural modal deformations and the performance achieved. The hardware testing, modal identification and structural reinforcements made on the prototype were described.

Current performance shows that the BSC-ISI is expected to provide the level of passive and active isolation required by aLIGO. The next steps will be to enhance the performance at low frequencies by limiting the horizontal seismometers tilt coupling and at high frequencies by pursuing the mitigation of structural resonances.

ACKNOWLEDGMENTS

LIGO was constructed by the California Institute of Technology and Massachusetts Institute of Technology with funding from the National Science Foundation and operates under cooperative agreement PHY-0107417. This document has been assigned LIGO Laboratory document number LIGO-P1000029.

REFERENCES

[1] B Barish, R Weiss. LIGO and the Detection of Gravitational Waves. Physics Today. 1999; 52: 44-50.

[2] B Abbott et al. LIGO: the Laser Interferometer Gravitational-Wave Observatory. Rep. Prog. Phys. 2009; 72 No 7: 25pp.

[3] G. M. Harry et al. Advanced LIGO: The next generation of gravitational wave detectors. Classical and Quantum Gravity, to be published in the Proceeding of the Eighth Edoardo Amaldi Conference on Gravitational Waves (2010).

[4] N A Robertson et al. Seismic isolation and suspension systems for Advanced LIGO. Gravitational Wave and Particle Astrophysics Detectors, Proceedings of SPIE. 2004; 5500: 81-91.

[5] R Abbott, et al. Seismic isolation enhancements for initial and advanced LIGO. Class. Quantum Grav. 2004; 21: 915-921.

[6] C. Hardham et al. Multi-DOF Isolation and Alignment with Quiet Hydraulic Actuators. Spring topical meeting on Control of Precision Systems, Proceedings of ASPE. 2004; 32: 127-132.

[7] N A Robertson, et al. Quadruple suspension design for Advanced LIGO. Class. Quantum Grav. 2002; 19: 4043-4058.

[8] W. Hua et al. Low Frequency Active Vibration Isolation for Advanced LIGO. Gravitational Wave and Particle Astrophysics Detectors, Proceedings of SPIE. 2004; 5500: 194-199.